

Spatial Variability of Sliding Plane on Volcanic Region. Case Study of STA 21+200 Cisumdawu Toll Road

Ahmad Kemal Arsyad¹, Martin Wijaya², Albert Johan¹, Paulus P. Rahardho^{2,*}

¹Research and Development Department, Geotechnical Engineering Consultant, Bandung, Indonesia, 40162; teknik@gec.co.id;

*Correspondence: paulus.rahardjo@unpar.ac.id

² Department of Civil Engineering, Faculty of Engineering, Universitas Katolik Parahyangan, Bandung, Indonesia, 40141

SUBMITTED 24 August 2023 REVISED 01 July 2024 ACCEPTED 26 July 2024

ABSTRACT Landslide can be caused either by natural phenomenon or due to human intervention. Regardless of the triggering factor, once landslide occurs, sliding plane in the form of discontinuity or sometimes referred as sliding plane is formed. Identifying the location and geometry of the sliding plane is important in determining the location of the reinforcement to rehabilitate slope failure. However, it is often difficult to locate the location and geometry of the sliding plane as the sliding direction is also difficult to ascertain. In this paper, slope failure which occurred in STA 21+200 of Cisumdawu toll road is used as case study. Variability of the sliding planes are investigated based on the location of the concrete overbreak that occurred during the bored pile construction on Tuff (volcanic soils) in Sumedang Region. Sliding planes are also estimated based on the soil investigation and pile boring records. The proposed solution is to reinforce the bored piles that did not penetrate into the hard layer with ground anchors installed at the pile cap.

KEYWORDS Landslide, sliding plane, slope failures, tuff, volcanic soils

1 INTRODUCTION

In December 2022, the Cisumdawu toll road on STA 21+200 experienced geotechnical problems related to landslides (Figure 1). There are presumptions that the cause of the slide was a material failure of the fill embankment which used tuff, a water-sensitive soil. The first geotechnical problem encountered was the damage of drainage channel made of box culverts. The damage was suspected to be caused by the movement of the embankment soil. Due to the damaged drainage channel, the flow of water became uncontrollable, further softening the embankment material and existing base soil, which is also consist of water-sensitive tuff.

The slope failure that occurred is considered complex due to the following factors:

- Difficulty in determining the cause of the landslide due to minimum data available;
- Soil conditions, fill and base materials consist of water-sensitive material;
- Deep boring data (soil investigation) does not show the weak plane.



Figure 1. Landslide in STA 21+200 Cisumdawu Toll Road

2 GEOLOGICAL CONDITIONS IN STA 21+200: VOLCANIC REGION

From the geological map of Bandung, it is known that the macro geological conditions of the STA 21+200 are in the Qyu formation (Figure 2), which means volcanic products, consisting of tuffaceous sand, lapilli, lava, agglomerates. The formation originated from Mount Tangkuban Perahu and Mount Tampomas. The area between Bandung – Sumedang, where the landslide occurred, is in a flat area or low hill area and is covered by reddish-gray and yellowish soil.

Tuff is a light color rock or soil (weathered rock or residual soil) and can exist in a vast state with no discontinuities. According to Asniar et al. (2019), tuff is made of volcanic ash with a particle size of less than 2 mm. Tuff has a high degree of cohesiveness due to the cementation that occurred during its formation (Asniar et al., 2019; Guan et al., 2001), but the cementation can deteriorate quickly due to water infiltration (Wedekind et al., 2012), making it particularly erodible (Letto et al., 2015). Tuff's shear strength may drop from 20% to 30% to up to 75% (Vasarhelyi, 2002; Price, 1983; Asniar et al., 2019).

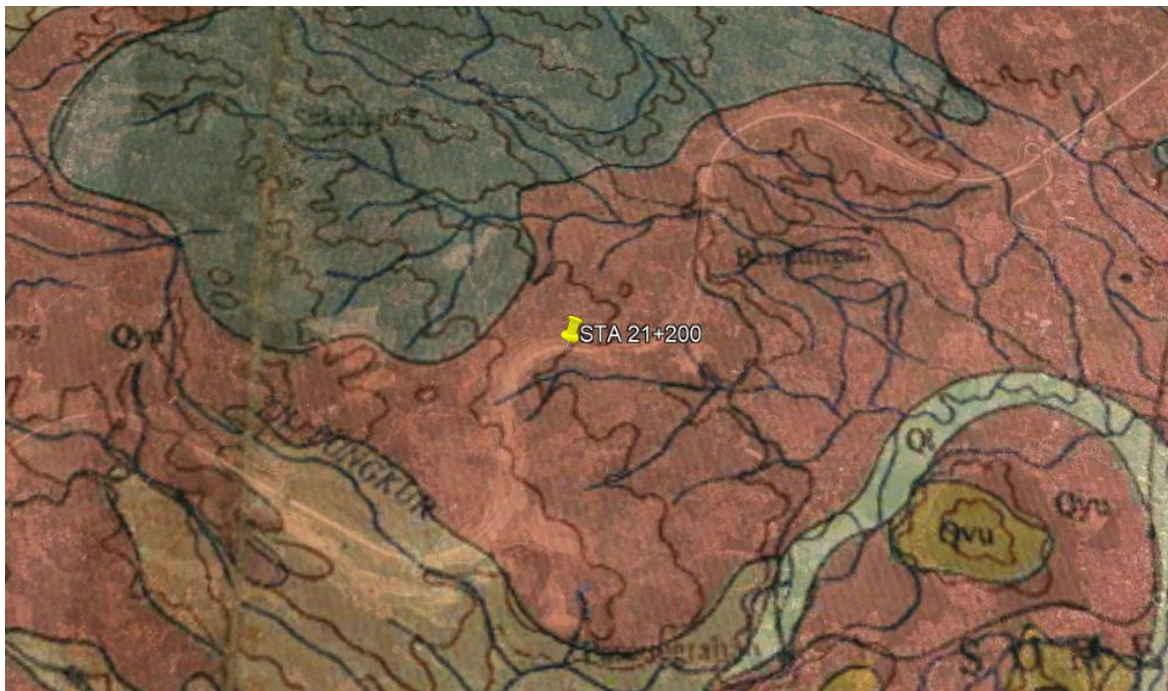


Figure 2. Landslide location on geological map of Bandung (Silitonga, 1973)

3 SOIL INVESTIGATION DATA

Soil conditions and stratigraphy are interpreted from soil investigation data in the field. There are two closest borehole data from STA 21+200, namely BH-16 and BH-17. The data shows that the soil layer is dominated by silt and clay layers. The hard soil layer ($N > 60$) is encountered at a depth of 35 m and 24 m for BH-16 and BH-17 respectively. The hard layer is made of Breccia, indicated as silt and gravel in the bore logs. The NSPT value of BH-16 and BH-17 is shown in Figure 3

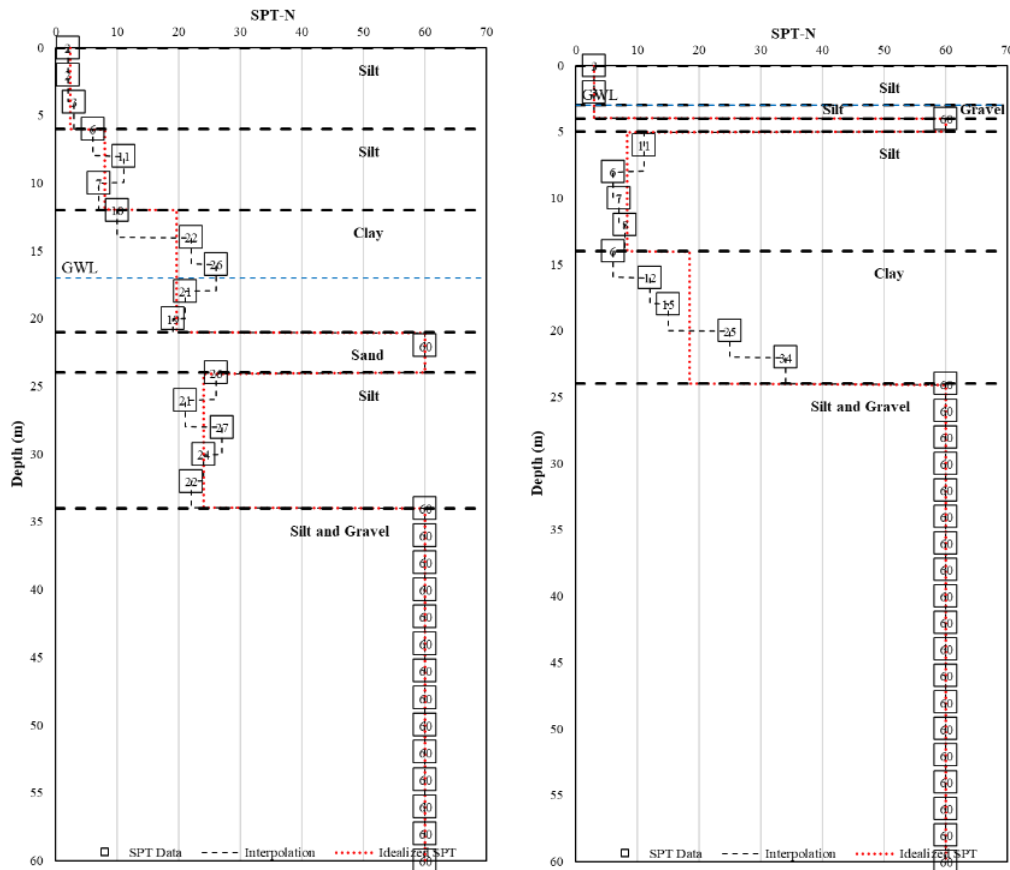


Figure 3. Closest borehole data from STA 21+200: BH-16 (left); BH-17 (right)

4 PROPOSED SOLUTION & PILE BORING RECORDS

The initial proposal was to construct a retaining wall consisting of soldier pile with a diameter of 0.8 m, a length of 26 m and a center-to-center (c.t.c.) spacing of 2 m. Regrading is also needed in front of the soldier pile by cutting and reducing the elevation by about 6 m. A 2D finite element model (Figure 4) was run to analyze the safety factor of the proposed design. The safety factor obtained was 1.43. Based on the application required, the safety factor is considered sufficient, and the proposed design is carried out in the field with 80 bored piles.

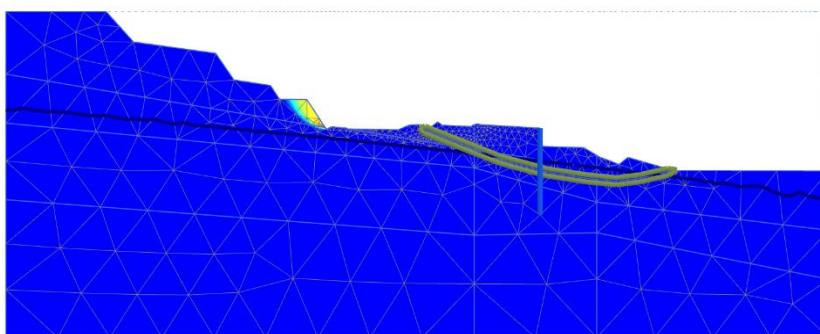


Figure 4. Safety factor of slope after soldier pile construction and reggrading (SF = 1.43)

4.1 Evaluation of Bored Pile Construction (29 August 2022)

By August 29, 2022, 25 bored piles have been constructed out of the 80 planned bored piles. Unusual observation was found. The number of bored piles that experienced overbreak (volume of concrete poured vs. theoretical concrete volume) was almost 50% (11 piles), 10 piles experienced overbreak

of 30-50%, and 4 piles experienced an overbreak of 10-30%. An overbreak can be an indication of bulging and can result in a reduction in the shear strength of the surrounding soil, which in turn causes a reduction in the carrying capacity of the bored pile.

Hard layer depth can be obtained by visual inspection of bored pile cuttings. From visual inspection, hard soil layer was not reached at 7 bored piles (BP-12, BP-23, BP-24, BP-27, BP-30, BP-33, BP-36) indicated by green circles in Figure 5.

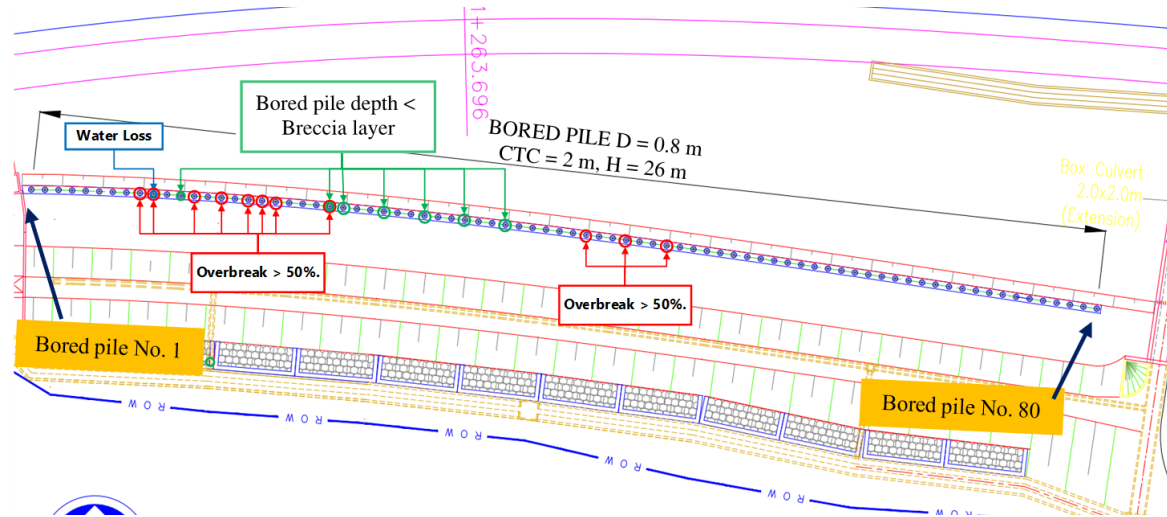


Figure 5. Mapping of constructed bored pile at STA 21+200 by 29 August 2022

From the pile boring records, it was suggested to increase the length of unconstructed bored piles (no. 46-80) to 36 m. The construction would resume by constructing indicator piles, which are pile numbered in multiples of 5. to the indicator piles were aimed to inspect the water loss and the depth of the hard layer for the 4 piles to be constructed between any two indicator piles.

4.2 Evaluation of Bored Pile Construction (17 September 2022)

After all the bored piles were constructed, it was found that the number of bored piles that experienced an overbreak of more than 50% were 28 piles, another 28 piles experienced an overbreak of 30-50%, and the last 24 piles experienced an overbreak of 10-30%. These findings can be an indication of the presence of weak soil layer.

Table 1. Summary of concrete *overbreak*

Overbreak Level	Number of Overbreak Piles	Bored Pile Number
> 50%	28	BP 10, BP 13, BP 19, BP 17, BP 9, BP 15, BP 18, BP 23, BP 42, BP 45, BP 48, BP 54, BP 25, BP 37, BP 43, BP 51, BP 35, BP 32, BP 29, BP 58, BP 41, BP 44, BP 47, BP 4, BP 7, BP 53, BP 56, BP 5
30% - 50%	28	BP 11, BP 21, BP 24, BP 27, BP 30, BP 12, BP 59, BP 33, BP 20, BP 28, BP 31, BP 34, BP 40, BP 38, BP 67, BP 50, BP 26, BP 36, BP 6, BP 49, BP 52, BP 8, BP 66, BP 80, BP 65, BP 2, BP 3, BP 1
10% - 30%	24	BP 16, BP 22, BP 14, BP 39, BP 57, BP 55, BP 61, BP 70, BP 60, BP 68, BP 73, BP 76, BP 69, BP 62, BP 78, BP 74, BP 71, BP 64, BP 77, BP 63, BP 72, BP 79, BP 75, BP 46

From the concreting logs, it is possible to estimate the depth of pile that experienced bad concreting in the form of bulging (enlargement) or necking (reduction). The level and depth of overbreak of the concrete can be used to identify areas where weakening of the soil layers may occur. Weakening of soil layers may be due to presence of soft, sandy soil with low shear strength. Bulging conditions were recorded on 76 piles with different levels of overbreak. On the other hand, necking conditions were recorded on 9 piles, namely BP 53, BP 57, BP 62, BP 66, BP 68, BP 69, BP 74, BP 75, BP 79.

Bulging or necking conditions can be illustrated with a graphical comparison of the theoretical concrete volume and the actual volume of concrete poured as shown in Figure 6.

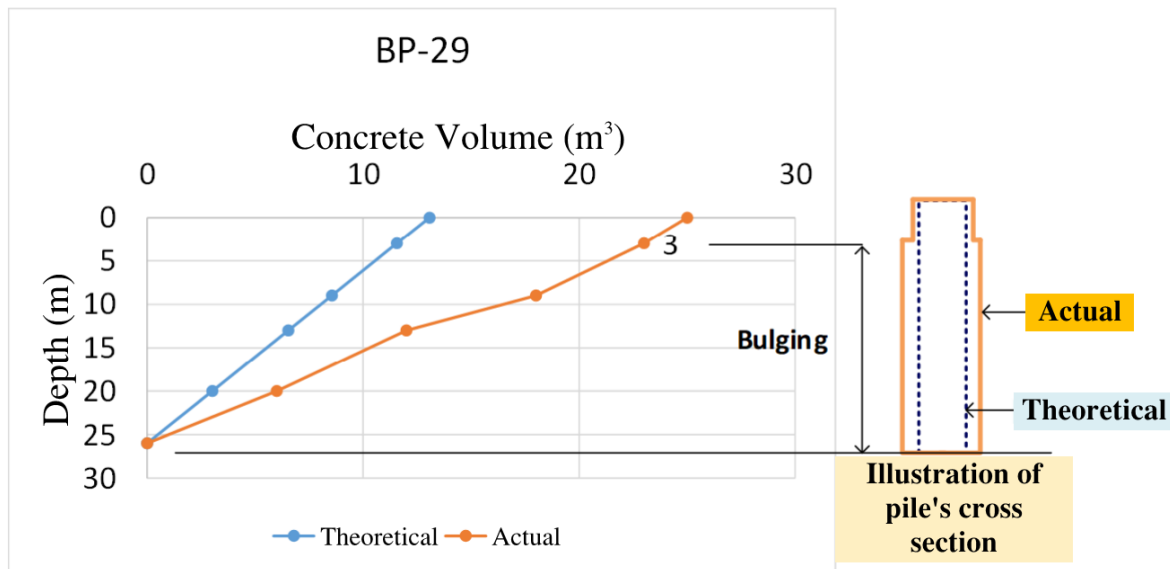


Figure 6. Graph of theoretical concrete volume vs. actual volume of concrete poured for BP 29 (88% concrete overbreak)

The most severe condition was recorded for BP 53, where necking occurred from the pile toe (36 m depth) to 10 m depth, followed by bulging until the pile head. The concrete overbreak for BP 53 is 153%. The graphical comparison of the theoretical volume and the actual volume of the concrete volume is shown in Figure 7.

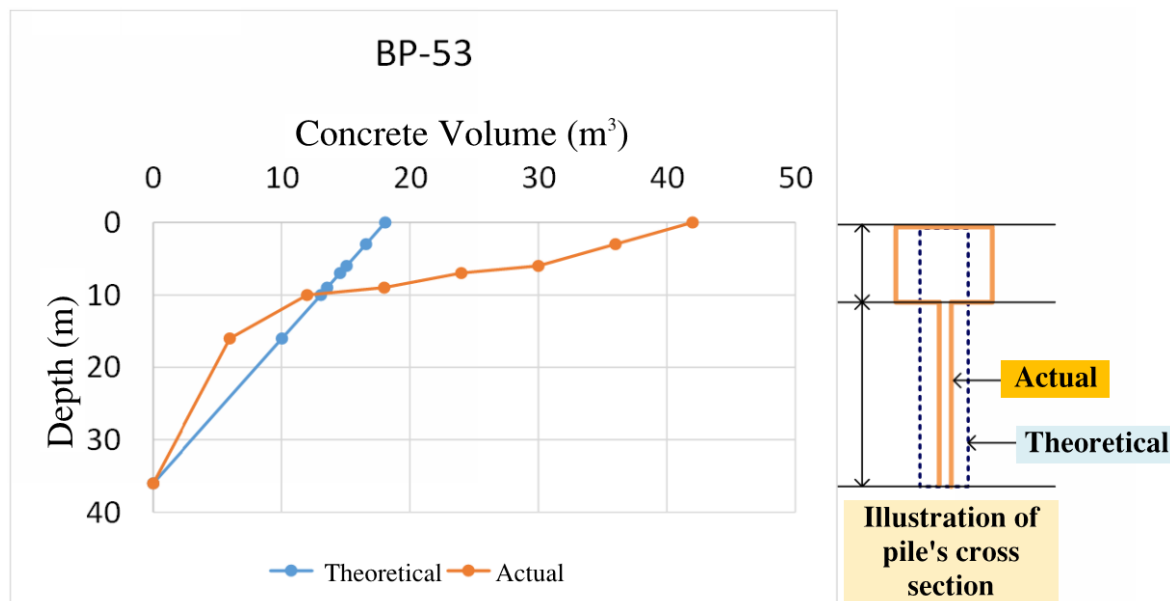


Figure 7. Graph of theoretical concrete volume vs. actual volume of concrete poured for BP 53 (131% concrete overbreak).

Figure 8 shows the concreting profile as well as the soil types from the drill cuttings. Bulging conditions are indicated by black block notations, while necking conditions are indicated by pink block notations (BP 53, BP 57, BP 62, BP 66, BP 68, BP 69, BP 74, BP 75, BP 79). The weak plane is estimated to be at the transition where concrete overbreak to non-overbreak occurred. The weak plane is found to be located at around 10-20 m from the ground surface.

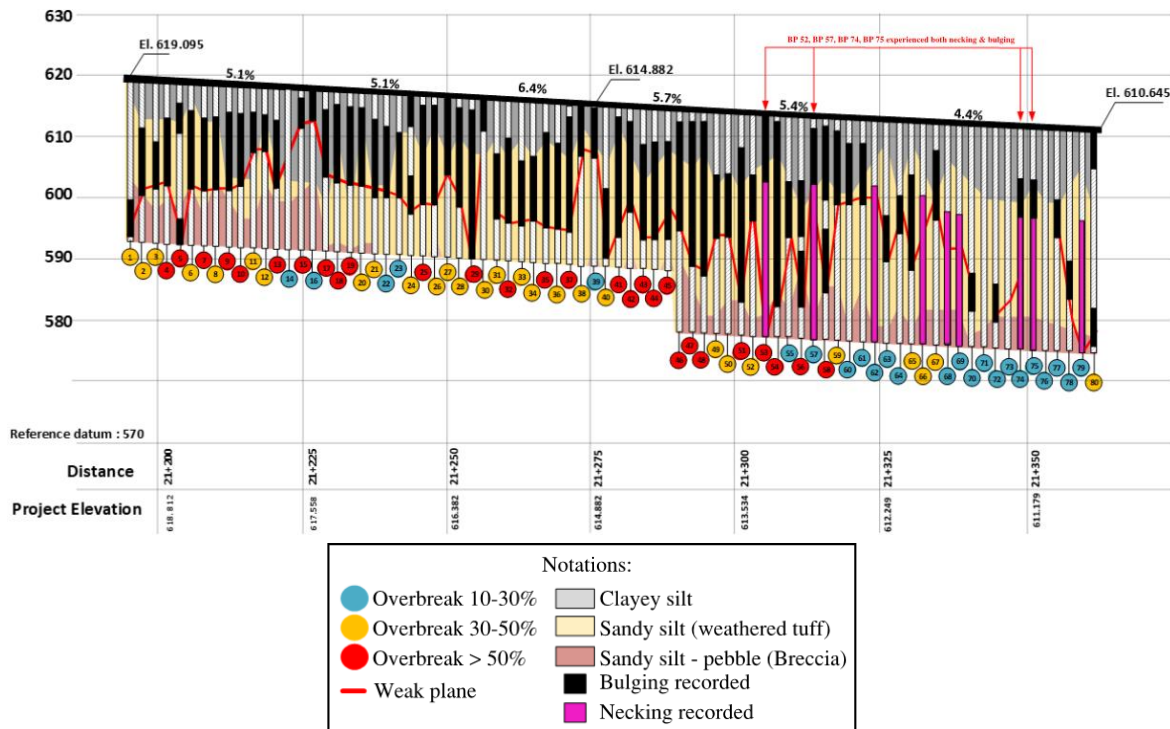


Figure 8. Soil Profile and Pile Condition Base on drilling record STA 21+200

5 MODELLING OF WEAK PLANE & REINFORCEMENT SOLUTION

5.1 Back Analysis of Weak Plane & Reevaluation of Previous Solution

With the new information from pile boring and concreting records, the previous slope model is reanalyzed to take into account the existence of weak plane. Figure 9 shows the position of the weak plane which is modelled as interface element. The soil properties in the soil element are then altered until safety factor of 1 is obtained. Based on the back analysis, the weak plane has a friction angle of 11 degrees and cohesion of 0 kPa.

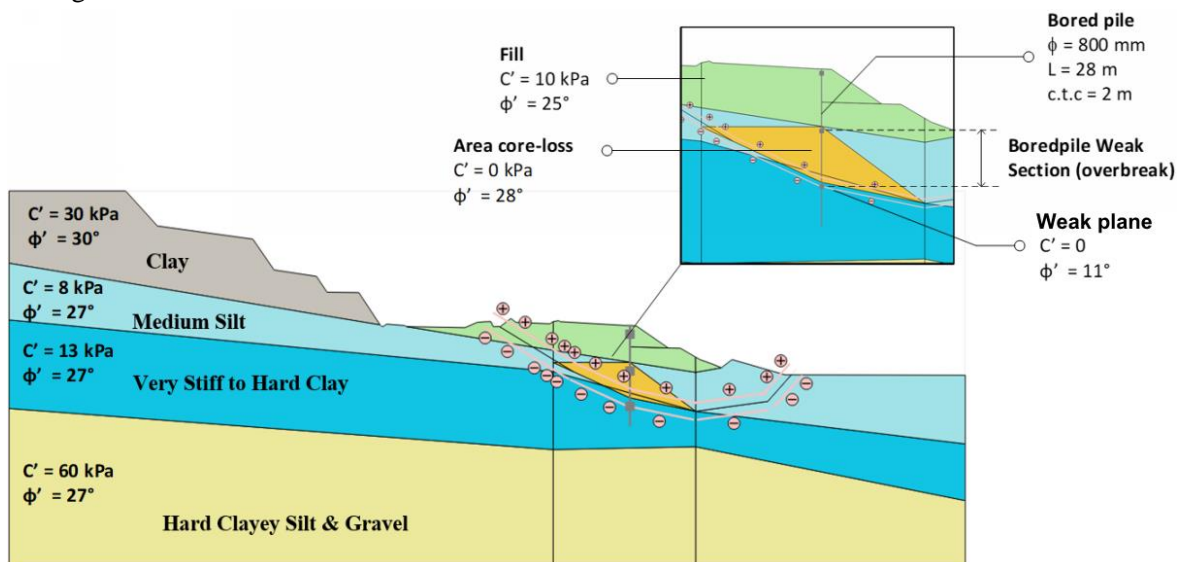


Figure 9. Back analysis of slope with weak plane (before failure)

After obtaining the properties of weak plane, the previous solution (with soldier pile) is re-analyzed with the weak plane modelled. The results show that the factor of safety dropped from 1.43 to 1.20, meaning the previous solution no longer meet the requirement specified in the Engineering Guideline for Handling Slope Collapses on Residual Soils and Rocks (Pd-T-09 2005 -B). Hence, reinforcement is required.

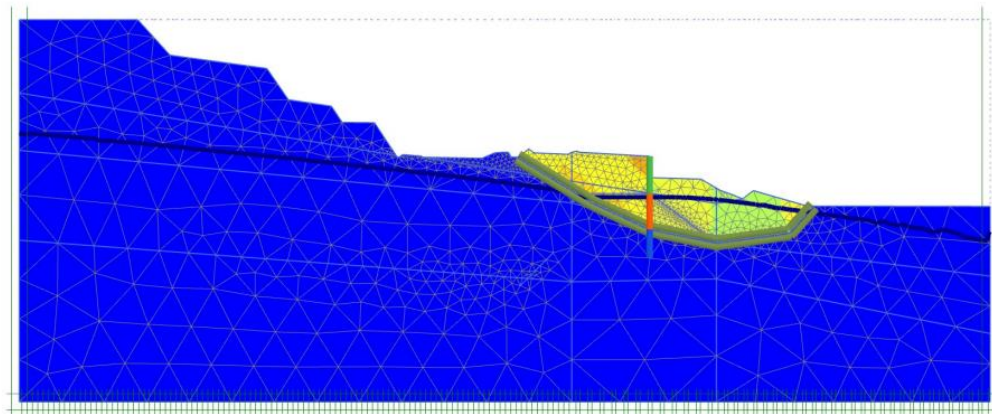


Figure 10. Reanalysis of solution with soldier pile considering the weak plane (SF = 1.20)

5.2 Reinforcement with Ground Anchors Installed on Pile Cap

From the authors' previous experience in other section of Cisumdawu Toll Road, the spatial variability of soil layers is quite high. If the worse-case scenario is taken from the soil investigation (BH 16), it would yield to uneconomical solution. Hence the design was based on the better results (BH 17). However, a contingency plan was planned ahead in the case the soldier pile solution is inadequate. The pile cap was preinstalled with pipes to allow addition of ground anchors when needed.

For the ground anchors to be effective, the ground anchors have to penetrate deeper than the weak plane, penetrating into the hard layer. Thus, the ground anchors length is chosen to be 38 m, with 25 m of free length (penetrating the weak plane), and bond length of 13 m. The ground anchors are to be installed at 45 degrees angle and a spacing of 4 m between anchors with 600 kN prestress are used. The details of the ground anchors are shown in Figure 11, and the finite element model is shown in Figure 12.

The result of soldier piles with ground anchors is shown in Figure 13. From the result, it can be seen that the slip surface has moved out of the piled area, just like the initial design (Figure 4). Hence the factor of safety returned to 1.43. Only bored piles not socketed into the hard layers are reinforced with ground anchors, namely BP 17 to BP 45. Figure 14 shows the area reinforced by the ground anchors.

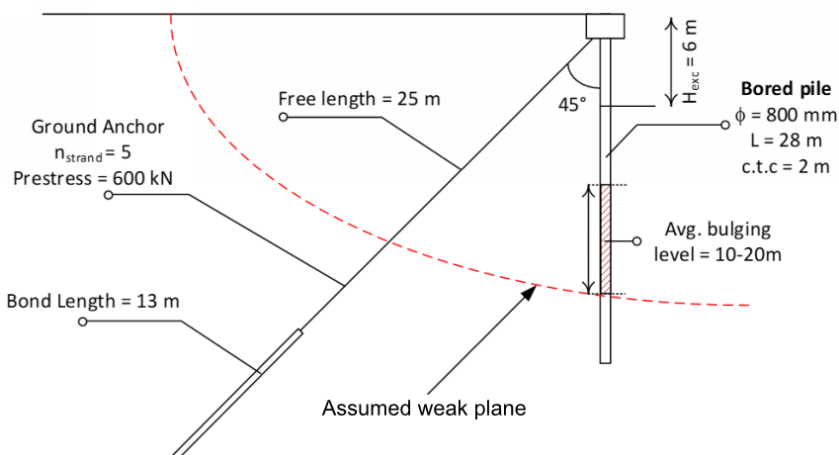


Figure 11. Details of ground anchor reinforcement

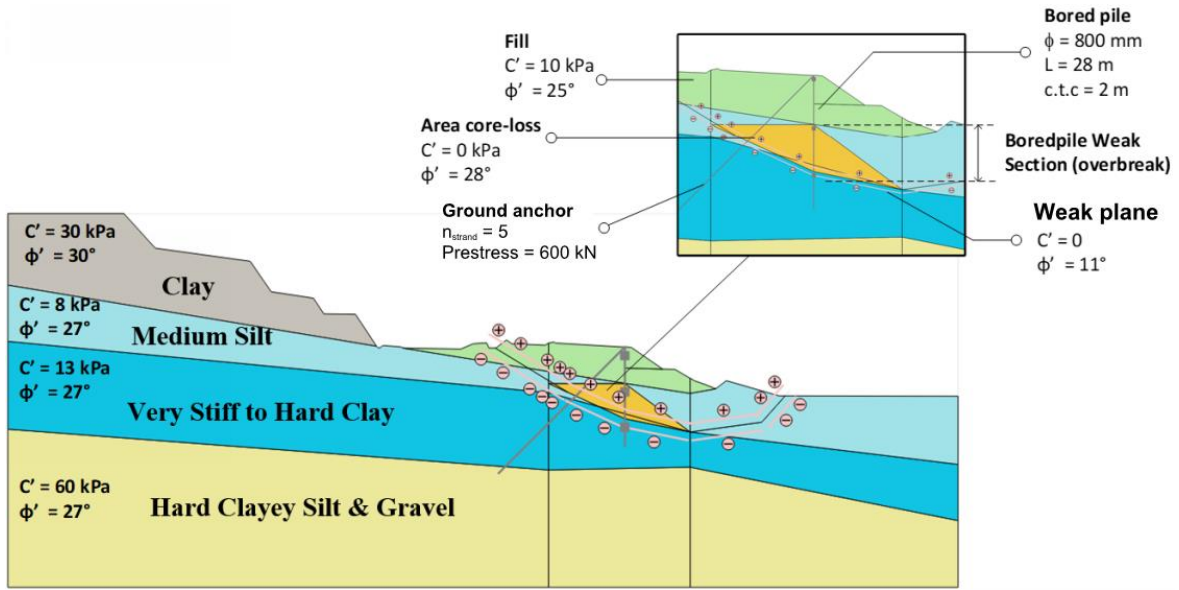


Figure 12. Plaxis 2D model of anchored bored piles

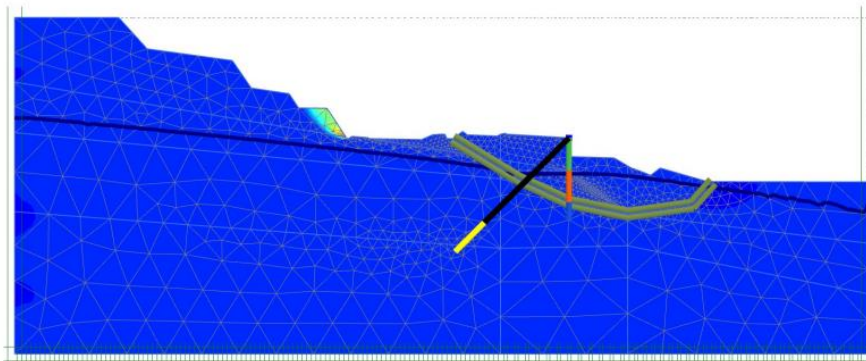


Figure 13. PLAXIS 2D output on bored piles reinforced with ground anchors (SF = 1.43)

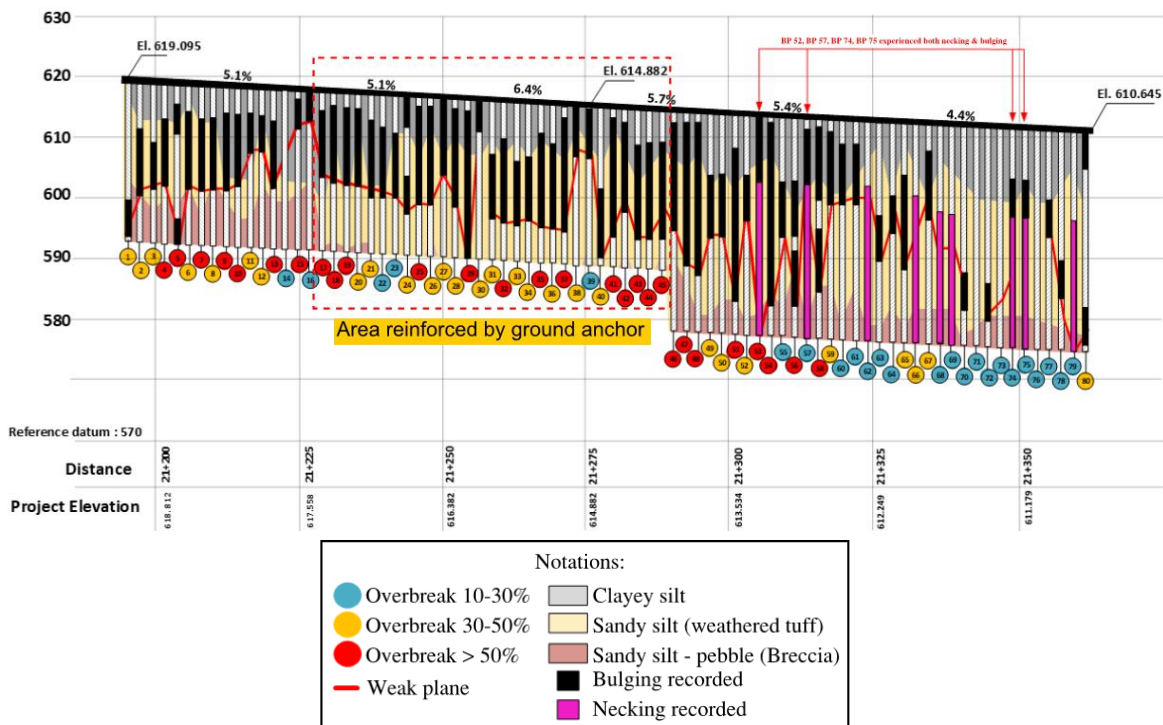


Figure 14. Section of bored piles reinforced using ground anchors

6 DISCUSSION AND CONCLUSIONS

A slope failure and its reinforcement that occurred in Cisumdawu Toll Road STA 21+200 is presented in this paper. The cause of failure is triggered due to a combination of embankment material and base soil which consist of tuff, a water sensitive soil. To enable the embankment to be built, reinforcement in the form of soldier piles is designed for. During the soldier piles construction, the spatial variability of the volcanic formation become apparent from the boring cuttings. Presence of weak planes also become apparent from the pile concreting records which show major concrete overbreak in most piles. Reanalysis of the soldier piles reinforcement with the presence of weak planes show that the factor of safety become inadequate. To improve the factor of safety, the soldier piles were further reinforced by using ground anchors.

This case study showcases the difficulties and challenges that can be faced when constructing embankment on volcanic region. The spatial variability of volcanic soils, heterogeneity infiltration pattern can trigger complex landslide behavior. Extensive site investigation is necessary to map the spatial variability of the volcanic formation. Only by knowing the spatial variability, an economical and safe solution can be designed for.

DISCLAIMER

The authors declare no conflict of interest.

ACKNOWLEDGEMENT

The authors would like to thank PT Geotechnical Engineering Consultant for the support which has been given and for providing the data, documentation and visual inspection at the site.

APPENDIX

Anggriawan, R., Salsabilla, N. A., & Prahesti, I. A. 2023. Volcanic Soils: Their Characteristics, Management Practices, and Potential Sollution for Water Pollution. *SEAS (Sustainable Environment Agricultural Science)*, pp. 18-29.

Asniar, N., Purwana, Y. M., and Surjandari, N. S., 2019. Tuff as rock and soil: Review of the literature on tuff geotechnical, chemical and mineralogical properties around the world and in Indonesia: AIP Conference Proceedings, v. 2114, no. 1, p. 050022.

Guan, P., Ng, C. W. W., Sun, M., and Tang, W., 2001. Weathering indices for rhyolitic tuff and granite in Hong Kong: *Engineering Geology*, v. 59, no. 1, pp. 147-159.

Letto, F., Perri, F., and Filomena, L., 2015. Weathering processes in volcanic tuff rocks of the "Rupe di Coroglio" (Naples, southern Italy): Erosion-rate estimation and weathering forms: *Rendiconti online della Società Geologica Italiana*, v. 33, pp. 53-56.

Price, R. H., 1983. SAND82-1314 Analysis of Rock Mechanics Properties of Volcanic Tuff Units from Yucca Mountain, Nevada Test Site: Sandia National Laboratories.

Rahardjo, H., Ong, T. H., Rezaur, R. B., and Leong, E. C., 2007. Factors Controlling Instability of Homogeneous Soil Slopes under Rainfall: *Journal of Geotechnical and Geoenvironmental Engineering*, v. 133, no. 12, pp. 1532-1543.

Sholehah, S. A., Karnisah, I., Suyono, A., & Budianto, B. S. 2020. Contribution of Rainfall To The Risk of Landslides at Cisumdawu toll Road Phase 3 STA 0+975 Case Study. *Advances in Engineering Research* (pp. 302-308). Bandung: Atlantis Press.

Silitonga, P. H. 1973. Geologic Map of Bandung Quadrangle, Java.) Direktorat Geologi.

Umbara, R., Indrawan, I. B., & Aldiamar, F. 2019. *Karakteristik Geologi Teknik dan Kestabilan Terowongan Sisi Kiri STA 12+628 hingga STA 12+654, Jalan Tol Cisumdawu - Jawa Barat*. Yogyakarta: Universitas Gajah Mada.

Vasarhelyi, B. 2002. Influence of the Water Saturation on the Strength of Volcanic Tuffs. *Workshop on volcanic rocks*, (pp. 89-95). Budapest.

Wedekind, W., López-Doncel, R. A., Dohrmann, R., & Kocher, M. 2012. Weathering of volcanic tuff rocks caused by moisture expansion. *Environmental Earth Sciences*, pp. 1203-1224.